



**HAL**  
open science

## **Analysis of multi-sensor, multi-spectral, active and passive imaging measurements.**

D. Hamoir, C. Grönwall, P. Lutzmann, E. Amselem, S. Barbé, M. Fraces, B. Göhler, H. Larsson, E. Repasi, O. Steinvall, et al.

► **To cite this version:**

D. Hamoir, C. Grönwall, P. Lutzmann, E. Amselem, S. Barbé, et al.. Analysis of multi-sensor, multi-spectral, active and passive imaging measurements.. 6th International Symposium on Optronics in Defense and Security (OPTRO 2014), Jan 2014, PARIS, France. hal-01059036

**HAL Id: hal-01059036**

**<https://onera.hal.science/hal-01059036>**

Submitted on 29 Aug 2014

**HAL** is a multi-disciplinary open access archive for the deposit and dissemination of scientific research documents, whether they are published or not. The documents may come from teaching and research institutions in France or abroad, or from public or private research centers.

L'archive ouverte pluridisciplinaire **HAL**, est destinée au dépôt et à la diffusion de documents scientifiques de niveau recherche, publiés ou non, émanant des établissements d'enseignement et de recherche français ou étrangers, des laboratoires publics ou privés.

# ANALYSIS OF MULTI-SENSOR, MULTI-SPECTRAL, ACTIVE AND PASSIVE IMAGING MEASUREMENTS

Dominique Hamoir <sup>(1)</sup>, Christina Grönwall <sup>(2)</sup>, Peter Lutzmann <sup>(3)</sup>,  
 Elias Amselem <sup>(2)</sup>, Stéphane Barbé <sup>(1b)</sup>, Michel Fracès <sup>(1)</sup>, Benjamin Göhler <sup>(3)</sup>,  
 Håkan Larsson <sup>(2)</sup>, Endre Repasi <sup>(3)</sup>, Ove Steinvall <sup>(2)</sup>, Bernard Tanguy <sup>(1)</sup>,  
 Emmanuelle Thouin <sup>(1)</sup>, Olivier Vaudelin <sup>(1)</sup>, Frank Willutsky <sup>(3)</sup>

<sup>(1)</sup> ONERA – The French Aerospace Lab, F-31055 Toulouse, France

<sup>(1b)</sup> ONERA – The French Aerospace Lab, F-13661 Salon de Provence, France,

Email: [dominique.hamoir@onera.fr](mailto:dominique.hamoir@onera.fr)

<sup>(2)</sup> FOI (Swedish Defence Research Agency), P.O. Box 1165, 583 11 Linköping, Sweden,

Email: [christina.gronwall@foi.se](mailto:christina.gronwall@foi.se)

<sup>(3)</sup> Fraunhofer-IOSB, Gutleuthausstrasse 1, 76275 Ettlingen, Germany,

Email: [peter.lutzmann@iosb.fraunhofer.de](mailto:peter.lutzmann@iosb.fraunhofer.de)

**KEYWORDS:** multi sensors sensing, active imaging, laser radar, IR imaging, SWIR imagers

## ABSTRACT:

We study the complementarity of active and passive EO sensors in different spectral bands, applied to friend or foe identification of human activities and of individuals. Laser imaging may complement radar or passive EO sensors. The laser may be fired only when required.

During field trials, we have recorded dynamic scenarios of interest with as many as ten sensors simultaneously: three active sensors in the NIR and SWIR regions, and seven passive sensors from the blue to the LWIR. The scenes include personnel using objects of interest, as well as reflectance and resolution targets. A good dataset was recorded, for distances from 600 to 1000 m, against different backgrounds and under a variety of atmospheric conditions.

These experimental data are under analysis to determine and understand the key phenomena that can be exploited for enhancing target-to-background discrimination and for defining sensor combinations of interest. We present first results.

## 1. INTRODUCTION

### 1.1. General introduction

The European Defence Agency (EDA) OB study ACTIM on active spectral imaging (2010-2011) [1, 2, 3], led Onera (France), Fraunhofer-IOSB (Germany) and FOI (Sweden) to understand the importance of live demonstrating the benefits of active imaging in complementing passive imaging.

We are especially interested in classifying and identifying humans, including the objects which they may hold and their associated activities. There is a rising military and security need for imaging systems for this purpose as situations of interest may be complex, with a mix up of friend or foe soldiers, combatants and civilians. The players may also operate in a variety of environments (rural, urban, mixed, sea, etc.).

In this context, WFoV (wide-field-of-view) radar or passive EO (electro-optic) sensors allow to monitor the scene and to pick individuals or objects of interest. NFOV (narrow-field-of-view) passive and active sensors zoom-in to determine their activities and recognise the types of objects and clothes they hold and wear. The benefits of operating simultaneously or consecutively in different spectral regions are already established and will be illustrated in this paper. One step further, the advantages of combining active sensing to passive imaging will be our main focus.

Passive panchromatic imaging in the visible (VIS), near-infrared (NIR), short-wave-infrared (SWIR), mid-wave-infrared (MWIR) and long-wave-infrared (LWIR) domains are mature solutions, with sensitive, large-format sensors now available in most bands, allowing for high performance WFoV sensors. Passive multi- and hyper-spectral imaging systems are maturing, with applications ranging from environmental monitoring and geology to mapping, military surveillance and reconnaissance. Data bases on spectral signatures allow for discriminating between different materials in the scene. However passive electro-optic sensors may be defeated under specific operational conditions to which active imaging may be less sensitive. For instance, active imaging offers a higher capability

to penetrate through atmospheric obscurants (fog, haze, smoke, dust, etc.) or to keep a high and constant target-to-background contrast whatever the natural lighting conditions (day/night, sunrise/sunset, shadows, etc.). Indeed, while passive multi- and hyper-spectral sensors rely on direct or indirect solar radiation, active sensors have the advantage of controlling the illumination. Especially for target identification (ID), it is therefore valuable to extend imaging systems to also include active sensing in spectral bands of interest. An extensive literature survey is given in our previous paper [4].

It is thus of interest to evaluate the performance of active and passive EO sensors and sensor combinations in classifying and identifying human targets, including their handheld objects and activities. It may open ways towards the design of optimised active/passive spectral imaging systems.

We have led a land campaign to collect input data [4]. We have combined as many as ten passive and active imaging sensors, in every spectral band: VIS, NIR, SWIR, MWIR and LWIR. All sensors did simultaneously record specially designed scenarios of human activities. The features of interest are the reflective signatures of the clothes, objects and backgrounds in the reflective domain, the emissive signatures of the persons and objects in the thermal domain, and the additional information brought to the human brain or to ATR (automatic target recognition) systems thanks to the movements of the targets. This results in an extensive database including ground-truth data. In our most recent communication we have detailed the conditions of the trials, given examples of images from the ten sensors involved and discussed the respective merits of 808 nm and of 1.5  $\mu\text{m}$  active imaging in the discrimination of clothes [4].

In this paper, in a first part we briefly introduce the trials. In a second part, we show the sensitivity of a few sensors to the environment, in particular to the atmospheric conditions. We give a few hints in

terms of complementarities between the different sensors. In a third part we compare the effects of turbulence on the resolution of comparable active and passive sensors. In a fourth and last part, we develop on the benefits of the "silhouette mode" capability of active sensors.

## 1.2. The field trials

The trials [4] were held on the Lima-Pirrène laser range of Onera (in Mauzac, Toulouse area, South of France). They took place on 8-12<sup>th</sup> April 2013. The laser range offers a rather flat grass-covered range of 1040 m (Figure 1). Many acts were plaid, with variations including the environment (weather, ambient light, turbulence), target range (600-1000 m), foreground and background (concrete at 1000 m, vegetation at short ranges), and first of all target features (clothes, handheld objects, morphology, posture, activity).

The ten sensors were operated simultaneously and from the same building, but up to 8 m apart. To be able to take care of the induced translation and rotation between sensors, flat geometrical targets (right side of the stage in Figure 1; designed to be seen in every wavelength) were used to enable an extrinsic calibration (registration) of the sensors. All clothes have been measured spectrally from 400 to 2500 nm. A spectrally calibrated reflectance board has been in every measured scene so that images from different sensors are calibrated to each other. A resolution target and a slanted-transition target were used to evaluate the spatial resolution and the sensor sight in different turbulence conditions. A scintillometer acquired the turbulence. Weather data and light conditions were also acquired. A fisheye camera monitored the clouds on 9th April 2013. Most scenes were also video recorded and/or photographed.

The teams and sensors involved in the trials were Onera (Gibi, Pelican, FLIR SC7000), FOI (Obzerv) and Fraunhofer-IOSB (Intevac, Xenics, AIM). The details of these ten sensors are given in Table 1.



Figure 1: The 1040-m-long laser range. The targets were located from 600 to 1000 m from the sensors.

Table 1: Characteristics of the imaging sensors involved in the field trials.

Instrument	Active/ Passive	Sensor	Wavelength coverage (nm)	FoV (mrad)	iFoV ( $\mu$ rad)	Frame rate (Hz)	NOHD (m)	eNOHD (m)
Gibi	Active	SWIR	1574	3 – 8.5	66.4 x 33.2	10	5 – 12	35 – 100
Pelican	Passive	Blue Green Red NIR	452 – 529 512 – 595 623 – 706 780 – 932	250	60	0.25	na	na
FLIR SC7000	Passive	LWIR	8000 – 9300	50	80	25	na	na
Obzerv	Active or Passive	NIR	808	8.4 – 146	13.2 – 12.2	30	20 – 108	140 – 756
Intevac	Active	SWIR	1572	17.1 x 12.9	26	20	2.4	9.6
Xenics	Passive	SWIR	900 – 1700	26.2 x 20.9	40.3	25	na	na
AIM	Passive	MWIR	3400 – 5300	15.4 x 11.5	22.3	30	na	na

### 1.3. Purpose and contents of this paper

Our final objective is to take advantage of the complementarities between spectral domains, as well as of the extra capabilities brought by active imaging as a complement to passive sensors. Our previous paper [4] described the trials and showed examples of results. In particular it compared active SWIR (Intevac) to both active and passive NIR (Obzerv).

The present paper reports additional analyses that could be readily performed from the data. In depth analysis and exploitation are planned for years 2014 and 2015. Here, we have decided to show and compare the effects of the environmental conditions on a few sensing modalities. We have chosen to present most of the spectral domains offered by WFoV and N FoV passive imaging: the NIR (Obzerv), the MWIR (AIM) and the LWIR (FLIR SC7000). Then we illustrate the performance obtained with N FoV active sensors. We focus on the active instrument Gibi as SWIR lasers are more "eye-safe" in the case of long-range applications requiring high emission powers. We also illustrate active NIR (Obzerv) that is suited to short-range applications and to applications where the hazard distance can be easily respected. See Table 1.

We have chosen a selection of appropriate scenarios among those recorded during the trials.

The conditions of every scenario discussed in the present paper are presented in Table 2.

Mist or rain induces a very good, lasting stability of the atmosphere, as in the evenings of 8<sup>th</sup>, 9<sup>th</sup> and 11<sup>th</sup> April 2013 with turbulence structure constant values ( $C_n^2$ ) not exceeding  $1.E-14 m^{-2/3}$ . The turbulence-induced image distortions are minimal for all systems and the scintillation speckles of the lasers are weak. All systems, in particular the active systems are at their best. Such conditions provide excellent single-frame images.

On the contrary, when the atmospheric turbulence is significant, both active and passive images are distorted by the propagation back to the sensor. In addition, active systems suffer from scintillation speckle. This speckle results from the coherent combinations occurring after the propagation of coherent light through an inhomogeneous medium.

For each sensor, we mainly illustrate these two extreme conditions, the first one resulting in images limited by the sensors only and the second one resulting in images limited by both the atmospheric perturbations and the sensor (sections 2-5). Meanwhile we show some specifics, advantages or limitations of each sensing modality.

We show the results under the same environmental conditions, detailed in Table 2, for every sensor.

Table 2: Details of the scenarios considered in this paper

Day	Time	Range (m)	C <sub>n</sub> <sup>2</sup> (m <sup>-2/3</sup> )	Condition	Global Irradiance (W/m <sup>2</sup> )	Temp (°C)	Relative Humidity (%)	Mean WS /10min	Mean WD /10min	Scenario
08/04/2013	19:17	600	1,5E-15	mist	70	12	60	0,4	306	chart
09/04/2013	17:23	600	1,2E-14	cloud & mist	224	14	58	0,5	246	gun
10/04/2013	17:28	1000	7,4E-14	clear	435	21	40	0,7	115	rifle
	23:07		4,6E-14		0	14	62	1,1	114	chart
	23:17		4,6E-14		0	14	63	1,8	121	rifle
11/04/2013	14:34	1000	4,4E-13	clear & humid	849	19	58	1,5	98	chart
	15:18		1,6E-13		712	20	57	1,5	114	plain silhouette
	20:16	600	5,7E-15	after rain	1	12	82	1,0	255	chart (moving)

We emphasize the two following conditions for which we present resolution evaluations with the bar-chart target. The very-low-turbulence data, with a C<sub>n</sub><sup>2</sup> value of 1.5E-15 m<sup>-2/3</sup>, at a range of 600 m, were recorded at sunset (blue characters in Table 2). The high-turbulence data, with a C<sub>n</sub><sup>2</sup> of 4.4E-13 m<sup>-2/3</sup>, at a range of 1000 m were recorded just after solar noon (red characters in Table 2).

The resolution is evaluated against the bar-chart. The wider bars are 100-mm wide and the scale factor between each bar group is  $\sqrt{2}$ . The ratio of length to width of all black bars is 5:1.

A specific section (section 6) on the so-called "silhouette mode" presents further situations when active sensing does nicely complement passive sensing. This opens up new operational capabilities in conditions when passive imaging would not be sufficient, enlarging the operability domain of the EO systems.

This analysis is complemented by a section (section 7) dedicated to the sensing resolution obtained with the active/passive NIR sensor Obzerv as a function of the atmospheric turbulence level.

## 2. PASSIVE NIR (Obzerv)

The NIR sensor from Obzerv is sensitive in a spectral domain (around 808 nm) where the signal is made of light reflected or diffused by the objects. Hence it can be operated either as a passive imager or as a gated-viewing active one. For better image quality, eye-safety, power consumption and covertness, its laser illuminator is fired only when the passive mode does not offer a sufficient SNR (signal-to-noise ratio).

In this section, we have chosen to detail only the passive mode of this NIR sensor, compatible with

daytime and sunset scenarios. This is however complemented by the section (section 7) dedicated to its sensing resolution as a function of the atmospheric turbulence level, both in passive and in active mode, and by a few active images in the section (section 6) dedicated to the "silhouette mode".

At sunset, atmospheric turbulence is very low. Figure 2 shows that, with an atmospheric turbulence structure constant C<sub>n</sub><sup>2</sup> of 1.5E-15 m<sup>-2/3</sup>, one can hardly resolve the finest pattern (most high-resolution) on the resolution chart, presenting a gap between bars of 13 mm, corresponding to an angular resolution of about 20 μrad at 600-meter range. We can clearly resolve about 25 mm gaps corresponding to an angle of about 40 μrad. The theoretical sensor limit is of about 11 μrad. The data present some blur due to turbulence and maybe focusing issues. There should be some room for image sharpness methods to improve the observed resolution.

At a range of 1000 m, close to solar noon on a clear day, under a high turbulence structure constant C<sub>n</sub><sup>2</sup> of 4,4E-13 m<sup>-2/3</sup>, the image (Figure 3) is very affected by atmospheric turbulence. It is hard to resolve the three most high-resolved patterns on the test chart.

In Figure 4a, under low turbulence, with a C<sub>n</sub><sup>2</sup> value of 1.2E-14 m<sup>-2/3</sup> at a range of 600 m, the person's clothes and cap look white, although they have other colours in reality, the gun is black. It is also possible to see the person's goggles. It is easy to identify the gun in this case, because of the difference in texture compared to both the person and the background. It is easy to recognise the person, the body parts and what action the person is performing. In Figure 4b, the resolution is degraded but the activity can still be recognised.

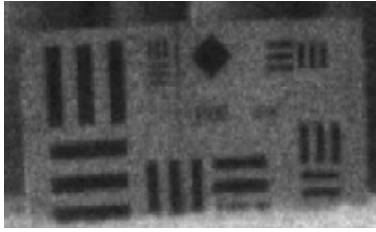


Figure 2: Passive NIR.  
Monday 08/04/2013, 19:17,  
resolution chart, 600 m,  $C_n^2$   $1.5E-15$  m<sup>-2/3</sup>.

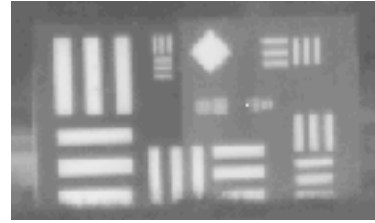


Figure 5: Passive MWIR.  
Monday 08/04/2013, 19:17,  
resolution chart, 600 m,  $C_n^2$   $1.5E-15$  m<sup>-2/3</sup>.

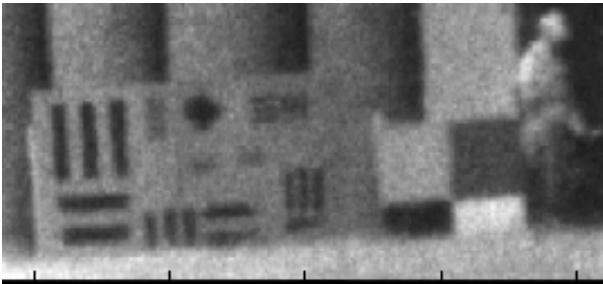


Figure 3: Passive NIR.  
Thursday 11/04/2013, 14:34,  
"resolution chart", 1000 m,  $C_n^2$   $4.4E-13$  m<sup>-2/3</sup>.



Figure 6: Passive MWIR.  
a) Thursday 11/04/2013, 14:34,  
"resolution chart", 1000 m,  $C_n^2$   $4.4E-13$  m<sup>-2/3</sup>.  
b) Wednesday 10/04/2013, 17:28,  
"aiming with rifle", 1000 m,  $C_n^2$   $7.4E-14$  m<sup>-2/3</sup>.

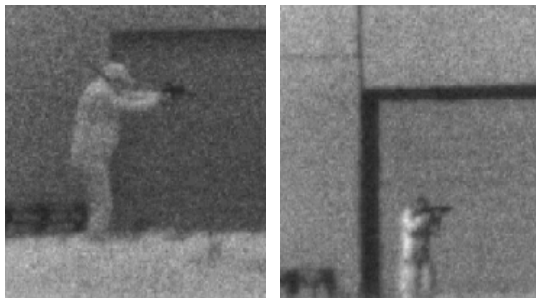


Figure 4: Passive NIR.  
a) Tuesday 09/04/2013, 17:23,  
"aiming with gun", 600 m,  $C_n^2$   $1.2E-14$  m<sup>-2/3</sup>.  
b) Wednesday 10/04/2013, 17:28,  
"aiming with rifle", 1000 m,  $C_n^2$   $7.4E-14$  m<sup>-2/3</sup>.



Figure 7: Passive MWIR.  
Tuesday 09/04/2013, 17:23,  
600 m,  $C_n^2$   $1.2E-14$  m<sup>-2/3</sup>.  
a) "aiming with gun".  
b) "person with gun close to his body".

### 3. PASSIVE MWIR (AIM)

The MWIR sensor from AIM is a thermal imager, sensitive from 3.4 to 5.3  $\mu\text{m}$ . In this spectral domain, the signal is dominated by the emissive contributions from the objects. This allows day/night operation. The sensor has an intrinsic resolution of 22  $\mu\text{rad}$ .

The data of Figure 5 correspond to the sunset conditions, when the atmospheric turbulence was very low. As was the case in the NIR domain (Figure 2), one can hardly see the finest pattern (most high-resolution) on the resolution chart. Some image processing may slightly increase the observed resolution.

Figure 6a on the bar-chart is very affected by atmospheric turbulence. It is hard to resolve the three most high-resolved patterns on the test chart. However the resolution looks better as compared to the NIR sensor, despite an iFoV (instantaneous field of view) of 22  $\mu\text{rad}$  as opposed to 12  $\mu\text{rad}$ . We may attribute this over-performance of the MWIR domain over the NIR domain to the longer wavelength that reduces the atmospheric effects.

The images of Figure 7 show a good contrast between the person's cap, jacket, trousers and skin. The gun can be seen clearly against the clothes, but it has similar texture as the metal door in the background. Therefore, when the person is

aiming with the gun, although one can see his hands, it is harder to see the actual gun. Again, it is easy to recognise the person, the body parts and what action the person is performing.

In the scene of Figure 6b, where there is more turbulence, all clothes and the rifle have the same texture. The rifle can be seen clearly against the background (a metallic door). The person's body parts and actions can be seen clearly.

#### 4. PASSIVE LWIR (FLIR SC7000)

The LWIR sensor FLIR SC7000 is a thermal imager, sensitive from 8.0 to 9.3  $\mu\text{m}$ . In this spectral domain, the signal is dominated by the emissive contributions from the objects. This allows day/night operation. With the lens that we have chosen for WFOV imaging with this camera, the resolution limit (diffraction limit  $\approx 100 \mu\text{rad}$  and geometric lens / detector combination  $\approx 80 \mu\text{rad}$ ) is two to six times higher than those of the other sensors. For this reason, the LWIR data should not be directly compared in terms of resolution to those generated with the other sensors. Because of the wide, 50-mrad field of view, the images are all cropped to the area of interest: the resolution chart, the other reference targets, the acting stage and their background (building or vegetation). Camera-embedded image corrections were activated from 10<sup>th</sup> April 2013, explaining why bad pixels appear in Figure 8 and 9 (like spread salt and pepper) whereas they are not visible in the subsequent LWIR images.

The resolution chart is a passive, reflective target designed primarily for sensors operating in reflective mode (visible, NIR and SWIR regions). During day-time, including sunset, the thermal contrast of the bar pattern against the metallic panel is good (Figure 8, Figure 9). It is even sufficient to observe the impact of atmospheric turbulence on the resolution of the LWIR sensing. Under these low turbulence conditions, with turbulence structure constants  $C_n^2$  of respectively  $1.5\text{E-}15$  and  $1.2\text{E-}14 \text{ m}^{-2/3}$  and a range of 600 m, one can just distinguish the third largest group of bars, corresponding to a resolution of 83  $\mu\text{rad}$ . This is consistent with the theoretical values.

Temporal and spatial fluctuations observed in Figure 10 and Figure 11, under high turbulence conditions, are particularly highlighted when video-playing the data. At a distance of 1000 m and with turbulence structure constants  $C_n^2$  of respectively  $7.4\text{E-}14$  and  $4.4\text{E-}13 \text{ m}^{-2/3}$ , one can hardly see the largest bars, corresponding to a resolution of 100  $\mu\text{rad}$ .

The observation of images at different hours shows an evolution of the thermal signature for the different components of the building (hangar door, walls, structures ...). The thermal signature of people changes much less. Therefore the passive LWIR contrast between the people and the background does change with time and depends strongly on the background element considered. In some cases, the contrast can be low enough (close to contrast inversion) to make it difficult to detect, recognize and/or identify the person. Indeed, Figure 12, under night-time conditions, a man handling a rifle is clearly visible, whereas in Figure 10, under day-time conditions, he is much more difficult to recognise due to the contrast reduction.

During night-time, the thermal contrast of the bar patterns is totally lost (Figure 12).

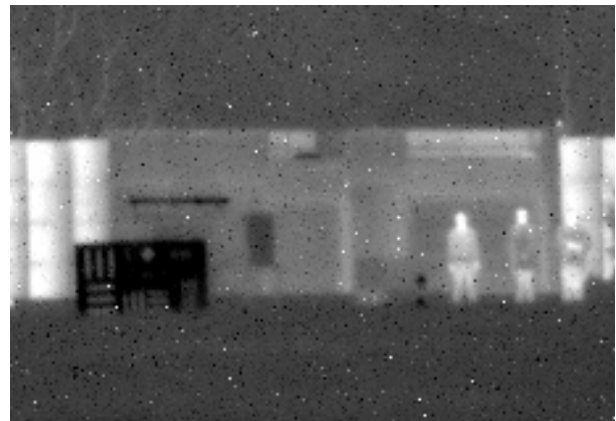


Figure 8: Passive LWIR.  
Monday 09/04/2013, 19:16,  
"resolution chart", 600 m,  $C_n^2$   $1,5\text{E-}15 \text{ m}^{-2/3}$ .

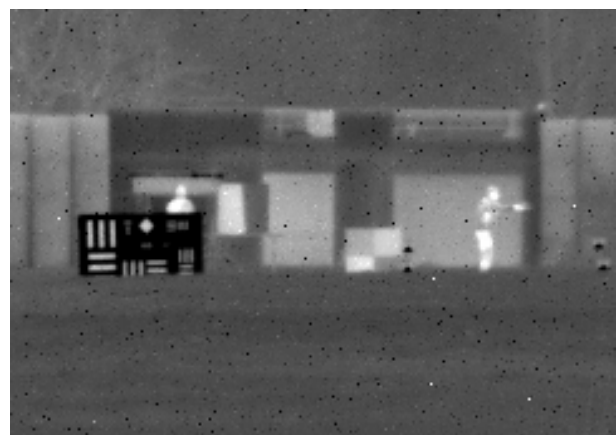


Figure 9: Passive LWIR.  
Tuesday 09/04/2013, 17:24,  
"aiming with gun", 600 m,  $C_n^2$   $1,2\text{E-}14 \text{ m}^{-2/3}$ .



Figure 10: Passive LWIR.  
 Wednesday 10/04/2013, 17:28  
 "aiming with rifle", 1000 m,  $C_n^2$   $7.4E-14$  m<sup>-2/3</sup>.



Figure 11: Passive LWIR.  
 Thursday 11/04/2013, 14:34,  
 "resolution chart", 1000 m,  $C_n^2$   $4.4E-13$  m<sup>-2/3</sup>.



Figure 12: Passive LWIR.  
 Wednesday 10/04/2013, 23:17,  
 "aiming with rifle", 1000 m,  $C_n^2$   $4.6E-14$  m<sup>-2/3</sup> ;  
 "contrast loss on the resolution chart".

## 5. ACTIVE SWIR (Gibi)

Active imaging with laser illumination of the scene offers advantages such as a total control over the illumination, an ability to penetrate through obscurants (thanks to the time-gating), an ability to operate day and night, and even at thermal inversion times, an ability to see in shadowed areas, etc.

Active imaging is possible in particular in the NIR and SWIR domains thanks to the reflection of light off the objects. The sensors may advantageously combine active and passive acquisition modes. The SWIR region is of particular interest as the laser light is invisible and relatively harmless. Further, the moon and the night-sky-radiance (or "night-glow", an atmospheric phenomenon that emits about five times more illumination than starlight) allow sensitive SWIR sensors to operate at night. Thus active/passive SWIR sensors may be of high interest.

The active signatures are constant as they rely on their reflective properties only. This is important to trained observers and ATR. Not only the signatures are constant but contrast-inversion or contrast-loss observed in Figure 12 in the LWIR are not expected. With fast moving targets, flash active imaging presents also the advantage of "freezing" the scene: there is no motion-blur.

In this section we present gated-viewing data acquired with the Gibi system, an active SWIR imager at the wavelength of 1574 nm. The sensor exhibits an intrinsic resolution of 33.2 x 66.4  $\mu$ rad (vertical x horizontal). During these trials we have operated Gibi in the active mode only. A spectral filter was used at reception in order to reject any ambient light during daytime. Note that the resolution and sensitivity of active SWIR imagers can be much better with last generation sensors.

Figure 13 and Figure 14 show data collected with the active SWIR Gibi system under low turbulence conditions. Figure 13 compares a single-frame image on the resolution chart at a 800-m range to the average image over five consecutive frames, under a turbulence structure constant  $C_n^2$  of  $1.5E-15$  m<sup>-2/3</sup>. Frame averaging does not significantly improve the resulting images under these conditions, as the turbulence-induced scintillation speckles are not resolved by the receiver of the instrument. In both cases one can hardly see the fifth largest horizontal bar pattern, corresponding to an angular resolution of 41  $\mu$ rad, but not the vertical ones. This is consistent with the theoretical limits of the instrument.

Figure 14 presents single-frame images on an individual using a hand-gun with aiming sight, at a 800-m range, under a turbulence structure constant  $C_n^2$  of  $1.2E-14 \text{ m}^{-2/3}$ . In the upper-left image, the person is surrounded by a light halo and his details are blurred due to some atmospheric diffusion by haze or mist in his vicinity (or at most a few tens of meters in front of him). A few minutes later, the second image is perfectly diffusion-free, as the haze or mist zone was local and passed by with wind. The third image is a zoom in the second image. It shows the level of details that could be observed, in particular the camouflage pattern, the cap and the gun.

Note in Figure 13 and Figure 14 the high target-to-background ratio offered in open-field conditions by gated-viewing. This advantage of active imaging is independent of the turbulence level.

Figure 15 presents single-frame and averaged SWIR Gibi images on a resolution chart located 1000 m from the sensors, under a turbulence structure constant  $C_n^2$  of  $4.4E-13 \text{ m}^{-2/3}$ . One can see the largest horizontal and vertical bars, corresponding to an angular resolution of  $100 \mu\text{rad}$ . It is difficult to evaluate whether  $50 \mu\text{rad}$  details could be distinguished if they were at the same altitude because the second largest bars are next to the ground (partly hidden and incurring maximum turbulence). We are reaching the turbulence-induced limits of this ground-to-ground SWIR active system over a flat terrain. These atmospheric degradations may be reduced by upgrading its components and design. Note also that a line-of-sight so close to the ground (1.30 m) over a 1-km free-space range is peculiar. In most operational cases the sensor may be placed upper from the ground (on a vehicle, mast, hill, building, etc.), the terrain may present some depression and/or the range may be restricted (urban theatre, vegetation, rocks, etc.). The benefits of the altitude of the sensor is well documented in [5].

Figure 15 and Figure 16 show that under such high-turbulence conditions, one gets a better visual appreciation when averaging frames (applying a median filter is slightly better). As the scene may not be static, a compromise should be sought and (with this sensor, under these conditions) may be obtained by both filtering over typically 5 frames and playing the video. Indeed, video visualisation does significantly improve the human perception of active images as the human visual system is extremely efficient at filtering out non-stationary noise such as speckle from stationary still or moving patterns (scene and targets).

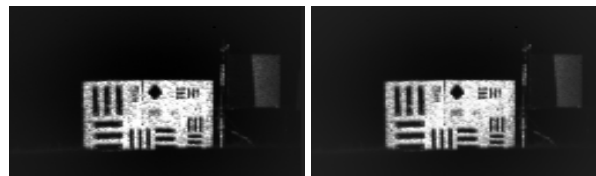


Figure 13: Active SWIR.  
Monday 08/04/2013, 19:17,  
"resolution chart", 600 m,  $C_n^2$   $1.5E-15 \text{ m}^{-2/3}$ .  
a) frame 33, b) average of frames 31-35.



Figure 14: Active SWIR.  
Tuesday 09/04/2013, 17:23,  
"aiming with gun", 600 m,  $C_n^2$   $1.2E-14 \text{ m}^{-2/3}$ .  
a) 17:23 (haze), b-c) 17:28 (no haze).

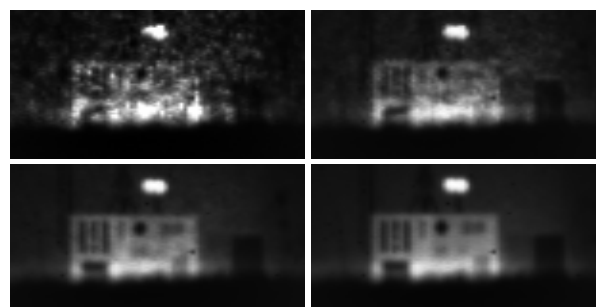


Figure 15: Active SWIR.  
Thursday 11/04/2013, 14:34,  
"resolution chart", 1000 m,  $C_n^2$   $4.4E-13 \text{ m}^{-2/3}$ .  
a) frame 578, b-d) averages of respectively  
frames 576-580, 550-590 and 301-607.

When time-filtering, textures such as camouflage patterns may be washed out when their characteristic dimensions do not exceed the frame-to-frame motion. A benefit from the observer point of view is that, when moving, a person wearing a

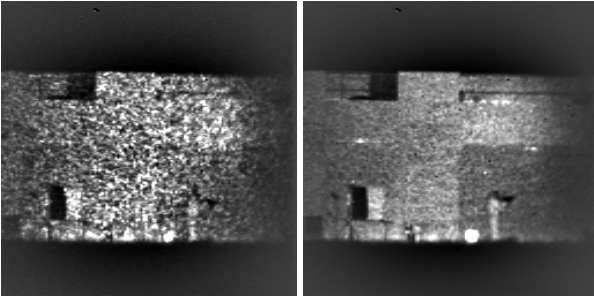


Figure 16: Active SWIR.  
 Wednesday 10/04/2013, 17:28,  
 "aiming with rifle", 1000 m,  $C_n^2$   $7.4E-14$  m<sup>-2/3</sup>.  
 a) frame 187, b) average of frames 190-199.



Figure 17: Active SWIR.  
 Thursday 11/04/2013, 20:16,  
 "removing targets", 600 m,  $C_n^2$   $5.7E-15$  m<sup>-2/3</sup>.  
 a) frame 678, b) average of three frames 678-680.

camouflage suit may be detected more easily with some averaging because the camouflage details would be washed out. On the contrary, his identification will be easier either without averaging or when he is still, because for identification the observer would be interested in the details of the person. Filtering may make loose tiny details such as camouflage but also armpits that a trained observer may identify on some of the single shots of the original video. Similarly, small objects held by the person will also be more easily identified when the target is still and with some temporal filtering.

Thus, on moving objects, averaging frames may degrade rather than improve the visualisation of moving targets. Averaging only two frames may even be worse than a single-frame image, because of the frame-to-frame movement. As an illustration, Figure 17 compares a single-frame image on the bar-chart to the average of three consecutive frames, when the chart was removed after the final scenario of the trials. Note the blurring of the uppermost and of the rightmost corners of the chart. This advocates for elaborated, adaptive image processing. Averaging or median filtering improves the perception of still scenes and targets, in particular by mitigating the scintillation speckles,

but when there is movement in the scene, the moving parts shall receive more appropriate treatments, and so when there are image distortions. A compromise may also be sought in increasing the frame-rate, with implications on the laser source that should be evaluated.

## 6. BENEFITS OF THE SILHOUETTE MODE

Remember in Figure 13, Figure 14 and Figure 17 the high target-to-background ratio offered by gated-viewing in open-field conditions, independent of the turbulence level. When the background is too close to the target to be rejected by an appropriate time-gating, the non-stationary scintillation clutter can be removed by temporal filtering, such as shown in Figure 15 and Figure 16, but a possible stationary background clutter would still be present, like in passive images.

Gated-viewing active systems offer the opportunity to shift their range-selective gate to behind the target, on the background. This is the so-called "silhouette mode". In this mode, the target and any object located in front of the range-selective gate appears black due to the absence of photons collected (as for objects located behind the gate), whereas the elements of the scene located within the gate, right behind the target, will show positive contrast and all their details.

Note that the silhouette mode does give an excellent target-to-background contrast, as shown in Figure 18, Figure 19 and Figure 20. In Figure 18, the automatic rifle is difficult to even detect in normal mode whereas it shows up and is easily identified with the silhouette mode. The same conclusion can be drawn from Figure 19.

However, as Figure 20 shows, the silhouette mode does not give information inside the contours of the target. Is the individual holding an object of interest? We are unable to answer the question unless the person moves so that his hands do not stay in front of his body. Hence, the silhouette mode is not self-sufficient and should come as a complement to standard gated-viewing.

In Figure 20, one also observes that averaging does not really improve the perception, as the contours of the silhouette are blurred by the averaging. On the contrary, silhouette-mode single-frame images are very appropriate in high turbulence conditions as the detection of the sharp contours of the silhouette is nearly immune to the scintillation speckle. The contours are only distorted (as passive images are).

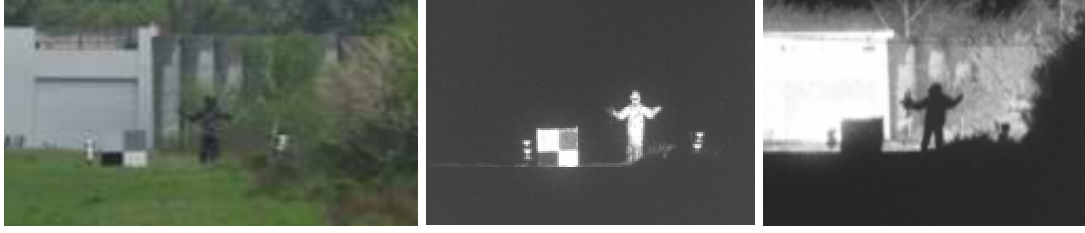


Figure 18: "soldier in uniform holding an automatic rifle in his right hand", range 600 m.  
a) photograph at short range, b) Active NIR (Obzerv) with gated-viewing,  
c) Active SWIR (Intevac) with silhouette mode.

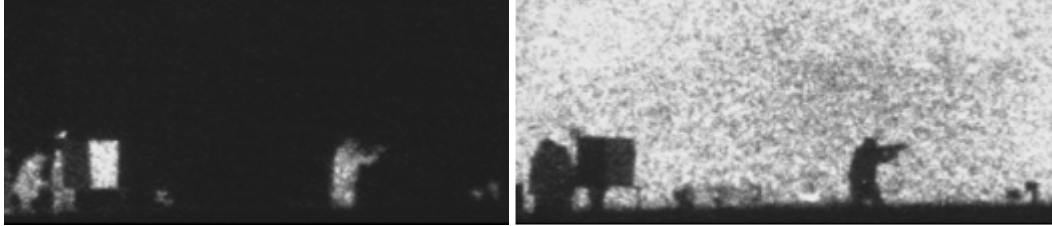


Figure 19: Active NIR (Obzerv). 10/04/2013, 1000 m.  
"person and black/white test target (left), and person aiming with rifle (right)".  
a) 23:13:31,  $C_n^2$  4.6E-14 m<sup>-2/3</sup>: gated-viewing;  
b) 23:17:40,  $C_n^2$  4.2E-14 m<sup>-2/3</sup>: silhouette mode.

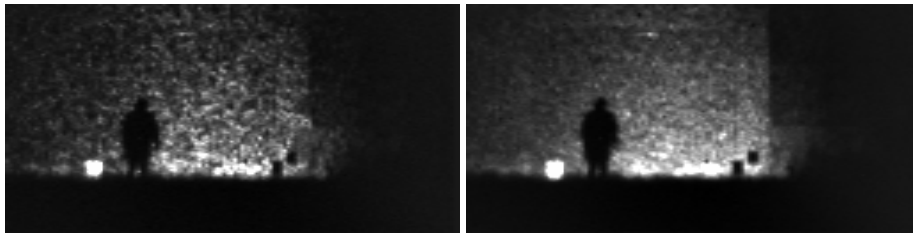


Figure 20: Active SWIR (Gibi). Thursday 11/04/2013, 15:18, 1000 m,  $C_n^2$  1.6E-13 m<sup>-2/3</sup>.  
silhouette mode: a) image 513, b) average of images 509-513.

The silhouette mode allows also to monitor the target with a high target-to-background contrast while keeping seeing the background, or even observing the backstage activity.

Figure 18 shows an example of the strong 1550 nm active signature in both reflective and silhouette mode. We are well aware that a range gated sensor is normally not a search sensor, nevertheless the strong signatures of persons as illustrated in Figure 18-20 may motivate that it is used for this purpose, either in the normal mode or in the silhouette mode, especially if the search sector is limited in size.

## 7. ESTIMATION OF THE EFFECTS OF ATMOSPHERIC TURBULENCE

We have investigated the angular resolution of the Obzerv imaging system according to the atmospheric turbulence level, both in passive and

active modes. The multi-bar resolution chart was used to determine the minimum resolvable bars from which a resolution angle could be estimated. The nominal instrument resolution is 11  $\mu$ rad for the 10.4-cm-aperture imager. The minimum observed resolution corresponds to the smallest bar pattern visible which was about 20  $\mu$ rad, obtained during low turbulence conditions ( $C_n^2 < 10^{-14}$  m<sup>-2/3</sup>). See Figure 2. For larger turbulence values the turbulent blur started to dominate. In this region the angular resolution can be approximated by  $\lambda/r_0$ , where  $\lambda$  is the wavelength and  $r_0$  the Fried parameter. Within the validity of the Rytov's method, i.e. within the non-saturated scintillation regime, the Fried parameter in the spherical wave approximation for the receiving path is given by:

$$r_0 = 2.1 \cdot \left[ 1.46k^2 \int_0^L C_n^2(z)(1-z/L)^{5/3} dz \right]^{-3/5} \quad (1).$$

$C_n^2(z)$  is the turbulence strength profile along the path from the target plane ( $z=0$ ) to the transmitter-receiver plane ( $z=L$ ) and  $k$  is the wave number,  $k=c/\lambda$ .

In Figure 21 we have plotted the estimated angular resolution for larger angles ( $>28 \mu\text{rad}$ ), where the turbulent blur is dominating, as a function of  $\lambda/r_0$ , with  $r_0$  calculated from the scintillometer data. The high scatter in data may be attributed to the uncertainties in the estimation of the angular

resolution, which was based on visual inspection of the bar patterns in single frames.

The angular resolutions for passive and active images are similar for equal turbulence levels which can be seen from Figure 22.

The active images could only be registered during darkness. During daytime, the daylight dominates over the laser illumination.

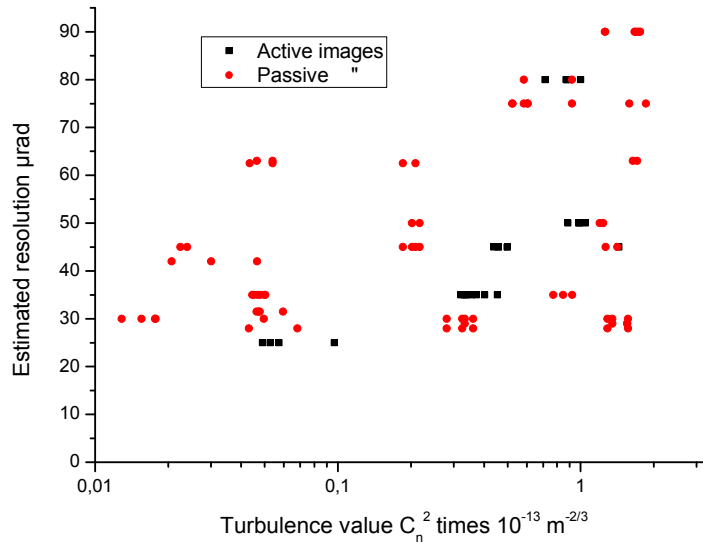


Figure 21. Angular resolution vs. turbulence strength for both active and passive images.

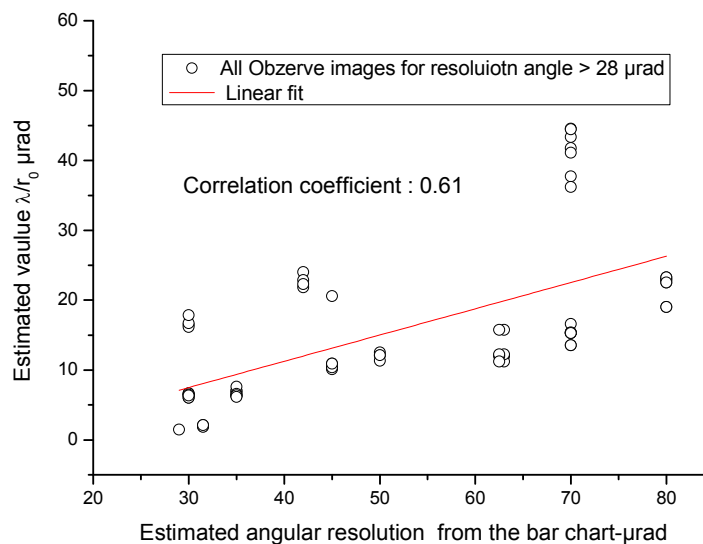


Figure 22. The estimated angular resolution from the bar patterns vs. the turbulence blur angle  $\lambda/r_0$  obtained from the scintillometer. Both active and passive images are included in the data.

## 8. CONCLUSION: COMPLEMENTARITY OF SENSORS

We study the complementarity of active and passive sensors in different spectral bands, applied to friend or foe identification of human activities and of individuals. Our work relies our field trial campaign of April 2013 [4].

The visual inspection of images from passive and active imaging sensors in the NIR, SWIR, MWIR and LWIR spectral regions (sections 2-5), indicates that all sensors give the ability to see the target and its movements at ranges up to 1000 m. All sensors do not always show details such as handheld objects and type of clothing clearly. However, usually at least one sensor can provide these details.

This encourages further studies on multi-spectral multi-sensor systems and on sensors operating in both active and passive mode.

With active imaging, the "silhouette mode" (section 6) gives an excellent target-to-background contrast and objects placed beside a person can be easily identified. However it does not give information inside the contours of the target, which indicates that the silhouette should come as a complement to standard gated-viewing. Further, silhouette-mode single-frame images are very appropriate in high-turbulence conditions as the detection of the sharp contours of the silhouette is nearly insensitive to the scintillation speckle. The contours are altered only by distortions (as passive images are).

We also made a study of the effects of atmospheric turbulence in the NIR region (section 7). The angular resolutions for passive and active images are similar for equal turbulence levels. We achieved high resolution images for both passive and active modes in high turbulence conditions also. The NIR active images could only be registered during darkness as daylight dominates over the laser illumination.

The initial analysis presented in this paper confirms that the extensive and ground-truth-calibrated database acquired during our field trials [4] (Mauzac, April 2013) is a good ground for further scientific studies including in-depth statistical analyses, validations of numerical modelling tools, observer tests, ATR tests and data fusion.

## 9. ACKNOWLEDGEMENTS

We greatly acknowledge all our sponsors.

The LIMA-Pirène site and equipments have been funded by ONERA, the Greater Toulouse Area, the Midi-Pyrénées Region and the European Union (FEDER program). The laser-range time has been offered by ONERA. The French participations in the field trial and in the analysis work have been funded by ONERA.

The Swedish participations in the field trial and in the analysis work have been funded by the Swedish armed forces FoT program and the Swedish Defence Material Administration (FMV).

## 10. REFERENCES

1. Steinvall, O., Ahlberg, J., Larsson, H., Letalick, D., Hamoir, D., Hespel, L., Boucher, Y., Déliot, P., Lutzmann, P., Repasi, E. & Ritt, G. (2011). Active Imaging (ACTIM), Report to the European Defence Agency ref. 09-R&T-008, restricted.
2. Hamoir, D., Hespel, L., Boucher, Y., Déliot, P., Steinvall, O., Ahlberg, J., Larsson, H., Letalick, D., Lutzmann, P., Repasi, E. & Ritt, G. (2011). Results of ACTIM, an EDA study on Spectral Laser Imaging, in Proc. SPIE. 8186, V81860M.
3. Steinvall, O., Renhorn, I., Ahlberg, J., Larsson, H., Letalick, D., Repasi, E., Lutzmann, P., Anstett, G., Hamoir, D., Hespel, L. & Boucher, Y. (2010). ACTIM: An EDA initiated study on spectral active imaging, in Proc. SPIE 7835, 78350C.
4. Grönwall, C., Hamoir, D., Steinvall, O., Larsson, H., Amselem, E., Lutzmann, P., Repasi, E., Göhler, B., Barbé, S., Vaudelin, O., Fracès, M., Tanguy, B., Thouin, E. (2013). Measurements and analysis of active/passive multispectral imaging, in Proc. SPIE 8897, 889705.
5. Steinvall, O., Elmquist, M., Chevalier, T. & Gustafsson, O. (2013). Active and passive short-wave infrared and near-infrared imaging for horizontal and slant paths close to ground, *Applied Optics* **52** (20), 4763-4778.